

Size-dependent same-material tribocharging in insulating grains

Scott R. Waitukaitis,¹ Victor Lee,¹ James M. Pierson,² Steven L. Forman,² and Heinrich M. Jaeger¹

¹ James Franck Institute and Department of Physics, The University of Chicago, Chicago, IL 60637

²Department of Earth and Environmental Sciences,
University of Illinois at Chicago, Chicago, Illinois, 60607

(Dated: September 10, 2022)

Observations of flowing granular matter have suggested that same-material tribocharging depends on particle size, rendering large grains positive and small ones negative. Models assuming the transfer of trapped electrons can explain this, but so far have not been validated. Tracking individual grains in an electric field, we show quantitatively that charge is transferred based on size between materially identical grains. However, the surface density of trapped electrons, measured independently by thermoluminescence techniques, is orders of magnitude too small to account for the scale of charge transferred. This suggests that another negatively charged species, such as ions, is responsible.

PACS numbers: 45.70.-n, 47.60.Kz, 37.20.+j, 51.10.+y

Although tribocharging is typically assumed to arise from frictional contact between dissimilar materials, it can also be caused by interaction between objects made of the same material. Several observations indicate that the mechanism for same-material tribocharging in granular systems is related to particle size, with larger grains typically charging positively and smaller ones negatively. The electric field of dust devils, for example, is known to point upward, consistent with smaller, negatively charged grains being lifted higher into the air [1]. A similar mechanism is suspected to be responsible for the large electric fields and consequent lightning generated in volcanic ash clouds [2–4]. Zhao *et al.* showed that the charge-to-mass ratio for a variety of powder samples crossed from negative to positive as the particle diameter increased, indicating a similar trend [5]. More recently, Forward *et al.* conducted experiments which revealed a correlation between charge polarity and grain size for samples with a binary particle size distribution [6–9].

Lowell and Truscott showed that dragging an insulating sphere across a plane (*i.e.* an “infinitely large” sphere) made of the same material usually caused the sphere to charge negatively [10]. They hypothesized that this behavior arises from a combination of asymmetry between two contacting surfaces and the transfer of trapped electrons [10, 11], which tunnel between surfaces when contact offers the possibility for relaxing into an empty, lower energy state. If the initial surface density of trapped electrons is uniform, continually rubbing some small region of contact (such as the tip of sphere) across a larger region (*e.g.* a plate) leads to net transfer of charge to the smaller region. Lacks and coworkers later showed how the same geometrical asymmetry also arises with random collisions among particles of different size [12–14]. However, while in most situations the transferred charge species is negative, there are some materials, such as nylon, where the polarity is reversed, which points to the possibility that other charge species might be responsible (Hu *et al.* recently suggested trapped holes might explain the polarity reversal [15]). Given these observations and

the lack of any quantitative data linking the amount of charge transferred to the density of trapped electrons, their role in same-material tribocharging is not certain.

To address this issue, we compare the net charge transferred between a binary sample of large and small grains to direct measurements of the initial trapped electron density as measured by thermoluminescence techniques. Our experiment for measuring both size and charge begins by mixing the granular material comprised of two grain sizes to initiate collisions. After placing the vessel of the mixed grains into a vacuum chamber, we open a small orifice at the bottom and allow the grains to flow freely from it via gravity (Fig. 1(a)). Grain interactions driving the charge transfer begin during mixing and continue until the grains leave the orifice and start free fall. The orifice size is chosen sufficiently small that the outflowing grains produce a dilute spray in which further collisions are rare. As the grains fall, they pass between two parallel, vertical copper plates held at potential difference V and separated by a distance l . The resulting electric field causes a grain of charge q and mass m to experience a horizontal acceleration $a = qV/ml$. Outside the chamber a high-speed, high-resolution video camera (Phantom v9.1, 1000 frames per second) guided by low-friction rails falls alongside the grains, which enables us to track their horizontal trajectories with precision. Performing approximately 25 camera drops at a given V we measure the acceleration of several thousand grains and construct acceleration distributions. From these data, we obtain an estimate of the minimum density of trapped electrons required to produce the observed charging. We then compare this estimate with direct measurements of the trapped electron density using thermoluminescence (TL), *i.e.* the emission of photons from the grains as heating them causes the trapped electrons to relax to lower energy states.

To ensure all grains are as materially identical as possible, we take particles from a single factory batch and sift the as-received particle size distribution (PSD) into several tight fractions. In the following, we focus on data ob-

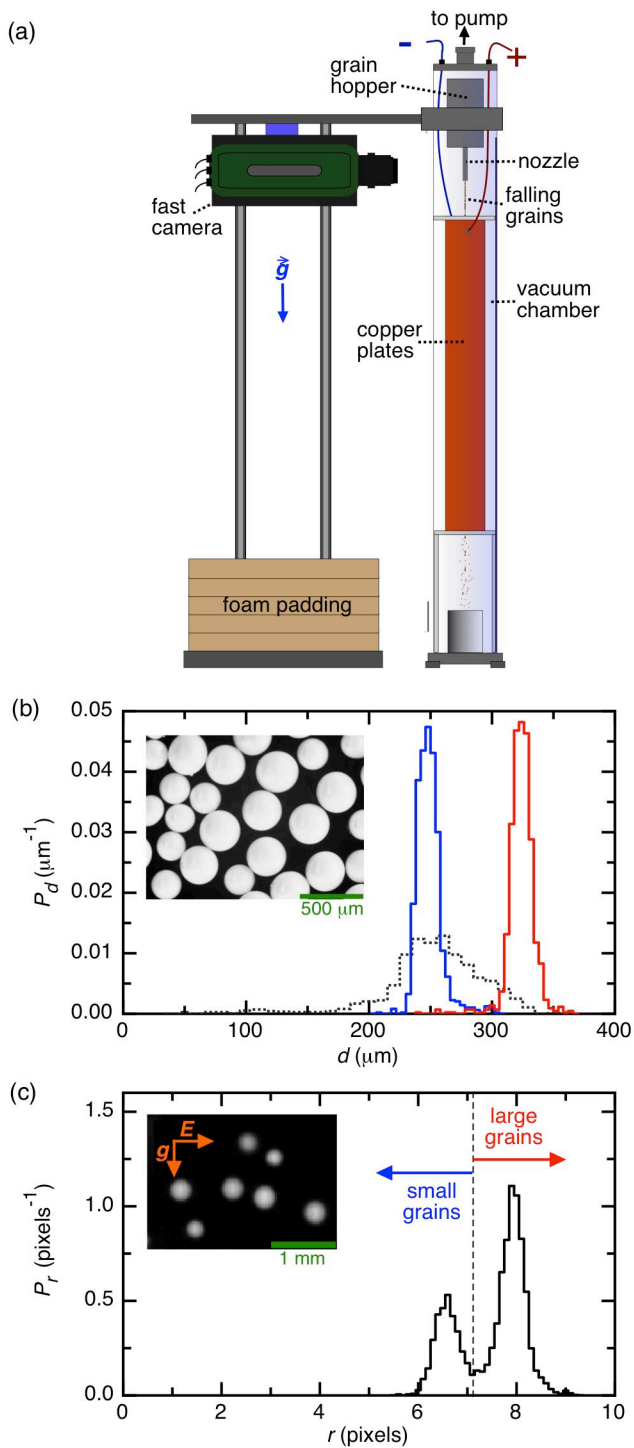


FIG. 1: (color online). (a) Schematic of setup for charge measurement by tracking particles during free fall in a horizontal electric field. (b) Normalized particle size distribution (PSD) determined by optical microscopy for unsifted grains (grey), sifted “small” grains (blue), and sifted “large” grains (red). Inset: optical microscope image of small and large grains together. (c) PSD of binary sample as determined by free-fall video imaging. Dashed vertical line indicates cutoff for deciding if a grain is counted as “large” or “small.” Inset: Still from video taken with the high-speed camera falling alongside the grains.

tained with fused zirconium dioxide - silicate ($\text{ZrO}_2:\text{SiO}_2$, Glenn Mills Inc.) as grain material because it exhibits strong charging behavior and because it is known to the TL community for its capacity to store trapped electrons [16–19]. For the experiments discussed here, we chose size cuts with average diameters $\bar{d}_l = 326 \pm 10 \mu\text{m}$ and $\bar{d}_s = 251 \pm 10 \mu\text{m}$ (Fig. 1(b)). As a baseline, we measured the average residual charge of the large and small grains before mixing with a Faraday cup [20], giving $\bar{q}_l = -(3.1 \pm 0.3) \times 10^4 e$ and $\bar{q}_s = -(5.9 \pm 0.7) \times 10^4 e$ per grain (here we take “e” to be the magnitude of the elementary charge, $+1.6 \times 10^{-19} \text{C}$). Next, we mixed the two sizes together in equal number by fluidizing them with nitrogen gas for approximately one half hour. The interior of the mixing vessel as well as its nozzle were coated with grains to prevent direct wall contact. After fluidization, the hopper was inserted into the main apparatus chamber, the chamber evacuated down to about 3 mTorr with a turbo pump, and the experiments performed as described above. For a more detailed description of the apparatus, see Ref. [21]. See [20] for an example high-speed video from the experiment.

In Fig. 2(a), we plot the acceleration distributions for the large and small grains at $V = 3.0 \text{ kV}$ ($|E| = 59 \text{ kV/m}$). As is clearly visible, the small grains (blue) have predominantly negative accelerations, *i.e.* negative charge, while the large grains (red) are predominantly positive. To extract the average charges \bar{q}_l and \bar{q}_s , we calculate the mean accelerations \bar{a}_l and \bar{a}_s for each size and plot them as a function of V , as in Fig. 2(b). The proportionality between \bar{a} and V confirms that the charge distribution is unaffected by the field and thus reflects the state of the sample as it exits the hopper (this proportionality would break down if particles collided and transferred charge inside the electric field, as in the field-induced dipole charging mechanism proposed by Pächt *et al.* [22]). From $\bar{a} = sV$, the slope $s = \bar{q}/l\bar{m}$ then gives access to the mean grain charge if the mass is known. Similarly, the width of the acceleration distribution, Δ_a , is related to the width of the charge distribution, Δ_q , via $\Delta_a = \sqrt{\delta_a^2 + (kV)^2}$, where $k = \Delta_q/l\bar{m}$ and δ_a is the average uncertainty in an individual acceleration measurement, independent of applied field.

From the specific material density $\rho = 3800 \text{ kg/m}^3$ and the PSD in Fig. 1b we compute the average grain masses as $\bar{m}_l = (7.0 \pm 1) \times 10^{-8} \text{ kg}$ and $\bar{m}_s = (3.1 \pm 0.8) \times 10^{-8} \text{ kg}$. Using the fit values for the slope s this leads to mean charges $\bar{q}_l = (1.8 \pm 0.2) \times 10^6 e$ and $\bar{q}_s = -(2.3 \pm 0.6) \times 10^6 e$ for the two particle sizes. For the widths we obtain $(2.9 \pm 0.4) \times 10^6 e$ and $(1.6 \pm 0.4) \times 10^6 e$ for the large and small grains, respectively. Note that the values for the mean charge are two orders of magnitude larger than the residual grain charge prior to mixing. Within our experimental uncertainties total charge is conserved, which makes it explicit that the charge transfer is occurring among the grains themselves and not with some other material (*e.g.* the container walls).

These data allow us to put a lower bound on the ini-

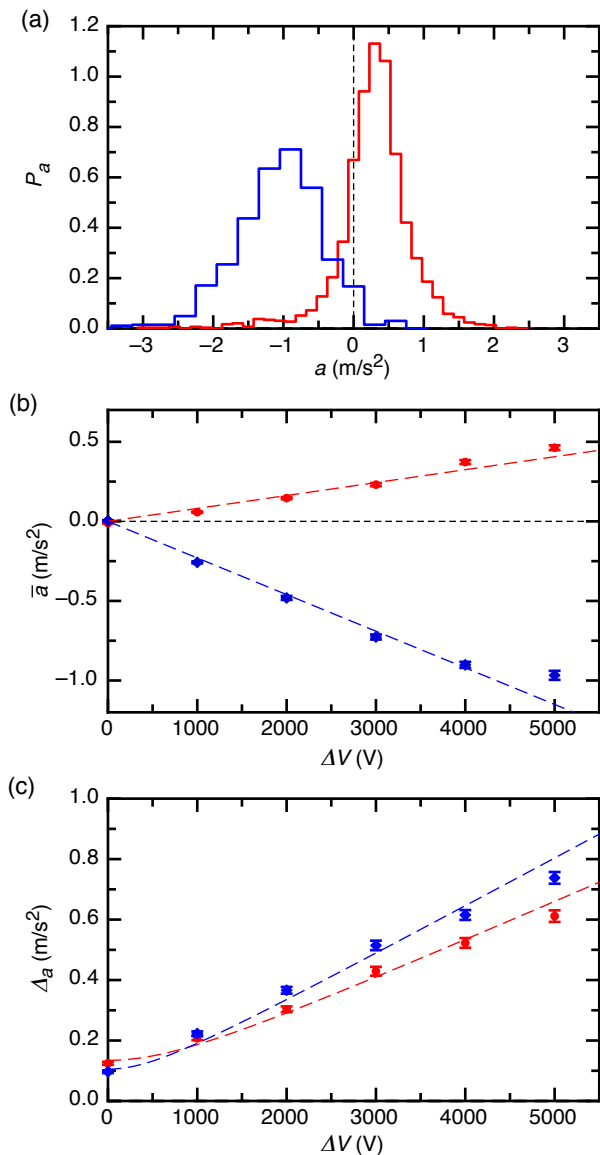


FIG. 2: (color online). Size-dependent charging. (a) Acceleration distribution of small (blue) and large (red) grains with $V = 3000$ V. (b) Mean acceleration \bar{a} of small (blue diamonds) and large (red circles) grains vs. V . Fits are of the form $\bar{a} = sV$. (c) Width of acceleration distributions Δ_a for small (blue diamonds) and large (red circles) gains vs. V . Fits are of the form $\Delta_a = \sqrt{\delta_0^2 + (kV)^2}$.

tial surface density of trapped electrons, σ . Assuming σ is the same for all grains initially and that *all* the excess trapped electrons of the large grains are transferred to the small grains, it must be the case that $\sigma > N/[\pi(d_l^2 - d_s^2)]$, where N is the total number of electrons transferred. Given the measured number of transferred charges $N \approx 2.0 \times 10^6$, this implies $\sigma > 15 \mu\text{m}^{-2}$. The randomness of collisions makes this “complete transfer” scenario unlikely and, using the results of Lacks *et al.* [13], a more realistic estimate is $\sigma > 90 \mu\text{m}^{-2}$.

To measure the actual density of trapped electrons in-

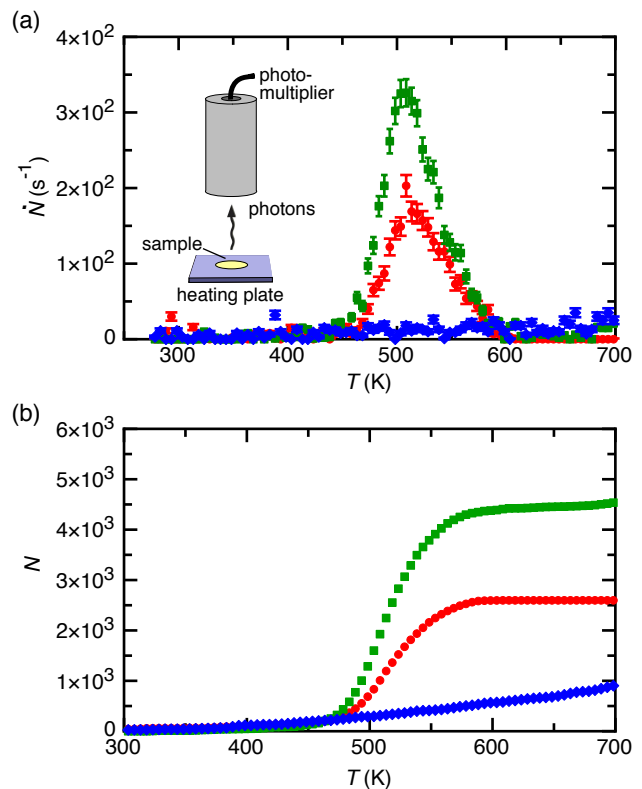


FIG. 3: (color online). Thermoluminescence (TL) measurements of trapped state density. (a) TL curves of photon count rate \dot{N} vs. temperature T at ramp rate 6 K/s for untreated grains (blue diamonds), grains exposed to ~ 12 hours sunlight (red circles), and grains exposed to ~ 12 hours UV lamp (green squares). Inset: schematic of TL measurement. (b) Total number of photons counted for same data as in (a).

dependently, we use a technique based on thermoluminescence. Trapped electrons on an insulating surface can be detected by heating the sample while simultaneously counting photons with a photomultiplier [23–25] [inset to Fig. 3(a)]. Each emitted photon corresponds to the relaxation of one trapped electron. Ramping the temperature ($T = T_0 + \beta t$) causes the emission rate \dot{N} to increase, but the population N is being depleted which leads to peaks in \dot{N} vs. T . In Fig. 3(a), we plot typical TL curves taken at a heating rate $\beta = 6$ K/s. For grains with no special preparation, identical to the ones used in the experiments of Fig. 2, we are unable to detect trapped electrons (the slight rise in the \dot{N} with T is a background “glow”). If we try to load electrons into the trap states by radiation, either from the sun or from an ultraviolet lamp, we observe one characteristic TL peak. As explained in [20], we can vary the heating rate to show that this trap has an energy below the conduction band $\epsilon = 0.36$ eV, typical for the trap depths encountered in other insulators [24].

In Fig. 3(b), we plot the integrated number of photons counted for each sample, which shows that even with maximum trap loading no more than ~ 5000 trapped

electrons were available. Accounting for the area of the sample and the geometry of our setup, the surface density of trapped electrons is approximately $\sigma = 2\pi N/A_s\Omega$, where Ω is the solid angle common to the sample (~ 5 sr) and the photomultiplier, and A_s is the area of the sample (~ 1 cm²). This reveals that the actual density of trapped electrons can be no more than $\sigma \approx 1 \times 10^{-4} \mu\text{m}^{-2}$, five orders of magnitude lower than the minimum necessary to account for the charge transfer we observed.

In principle, it is possible that additional electrons exist at trap depths deeper than we can reach with the temperature range available to us, but several factors make this unlikely. First, although our TL measurement should be sensitive to traps as deep as ~ 2 eV (provided the surface density of these traps $\sim 15 - 90 \mu\text{m}^{-2}$, as our charging data implies), we see no indication of traps beyond the one at $\epsilon \sim 0.36$ eV. Additionally, traps beyond ~ 2 eV would be especially deep compared to what is typically reported in the literature [24]. More importantly, if traps did exist in this range, they would be susceptible to unloading via visible light ($\sim 1.8 - 3.1$ eV). This point is especially relevant to granular systems continually exposed to visible light from the sun, such as wind-blown dust or volcanic ash, which also exhibit strong, same-material tribocharging behavior [1–4, 26–29].

Our finding of strong same-material tribocharging in grains where we can effectively rule out trapped electrons as the source highlights an ongoing debate regarding the most fundamental question in tribocharging: what is the charge species being transferred? While in metal-metal tribocharging it has been shown that electrons are transferred [30, 31], insulator-insulator experiments have pointed to electron transfer [32–34], transfer of ions adsorbed on the surface [35–38], and recruitment of ions from the atmosphere surrounding the contact [39]. In our case, where the charge transfer involves a negatively charged species and trapped electrons are not the culprit, this points to ions.

Baytekin *et al.* recently performed detailed experiments with different insulating materials where they employed both Kelvin force microscopy (to measure the spatial charge distribution) and confocal Raman spec-

troscopy (to spatially resolve chemical signatures) to reveal that charge transfer is correlated with the breaking of molecular bonds and subsequent transfer of charged molecular groups between surfaces [37]. Several studies have pointed out [35, 36, 40] the particular importance of molecularly thin layers of adsorbed water. As discussed by McCarty and Whitesides for nonionic polymer surfaces, in such 1-2 nm thin films the water segregates and the hydroxide (OH^-) tends to accumulate in the Stern layer at the solid surface, while the hydronium (H^+) remains mobile. These authors suggest that in this case contact charging is due to the transfer of OH^- ions [36]. Since some moisture will adsorb almost instantaneously, even on nominally hydrophobic surfaces, unless a sample is prepared and maintained under ultra-high vacuum, OH^- ions could easily be responsible for the results we observe. Specifically, given that the geometric arguments associated with contact asymmetry in the Lowell/Truscott/Lacks model are independent of the origin of the charge species, the tendency of large (small) particles to charge positively (negatively) would arise equally well with the transfer of OH^- ions in place of trapped electrons. The only requirement would be the availability of surface sites to accept transferred OH^- , similar to the availability of empty low-energy states in the trapped electron model. In this scenario, the density of transferrable charges is no longer an issue: even with partial monolayer coverage the number of OH^- ions far exceeds the lower bound of $15 \mu\text{m}^{-2}$.

We thank Gustavo Castillo, Estefania Vidal, Suomi Ponce Heredia, and Alison Koser for contributions during the early stages of setting up the free-fall experiment, and Daniel Lacks, Troy Shinbrot, Ray Cocco, and Ted Knowlton for discussions. This work was supported by the NSF through DMR-1309611. Access to the shared experimental facilities provided by the NSF-supported Chicago MRSEC (DMR-0820054) is gratefully acknowledged. S.L.F. and J.L.P. acknowledge funding from UIC NSF Grant No. 0850830 and 0602308. S.R.W. acknowledges support from a University of Chicago Millikan Fellowship and from Mrs. Joan Winstein through the Winstein Prize for Instrumentation.

-
- [1] J. R. Leeman and E. D. Schmitter, *Atmos. Res.* **92**, 277 (2009).
 - [2] M. Brook, C. Moore, and T. Sigurgeirsson, *J. Geophys. Res.* **79**, 472 (1974).
 - [3] R. Anderson, S. Gathman, J. Hughes, S. Bjornsson, S. Jonasson, D. Blanchard, C. Moore, H. Survilas, and B. Vonnegut, *Science* **148**, 1179 (1965).
 - [4] T. Mather and R. Harrison, *Surv. Geophys.* **27**, 387 (2006).
 - [5] H. Zhao, G. Castle, and I. Incelet, *Journal of Electrostatics* **55**, 261 (2002).
 - [6] K. M. Forward, D. J. Lacks, and R. M. Sankaran, *J. Electrostat.* **67**, 178 (2009).
 - [7] K. M. Forward, D. J. Lacks, and R. M. Sankaran, *Geophys. Res. Lett.* **36**, 1 (2009).
 - [8] K. M. Forward, D. J. Lacks, and R. M. Sankaran, *Ind. Eng. Chem. Res.* **48**, 2309 (2009).
 - [9] K. Forward, D. Lacks, and R. Sankaran, *Phys. Rev. Lett.* **102**, 028001 (2009).
 - [10] J. Lowell and W. Truscott, *J. Phys. D. Appl. Phys.* **19**, 1273 (1986).
 - [11] J. Lowell and W. Truscott, *J. Phys. D Appl. Phys.* **19**, 1281 (1986).
 - [12] D. J. Lacks, N. Duff, and S. K. Kumar, *Phys. Rev. Lett.* **100**, 188305 (2008).
 - [13] D. Lacks and A. Levandovsky, *J. Electrostat.* **65**, 107

- (2007).
- [14] N. Duff and D. Lacks, *J. Electrostat.* **66**, 51 (2008).
- [15] W. Hu, L. Xie, and X. Zheng, *Appl. Phys. Lett.* **101**, 114107 (2012).
- [16] P. Lacconi, D. Lapraz, and R. Caruba, *Phys. Stat. Sol. A* **50**, 275 (1978).
- [17] W.-C. Hsieh and C.-S. Su, *J. Phys. D Appl. Phys.* **27**, 1763 (1994).
- [18] H. Hristov, N. Arhangelova, V. Velez, I. Penev, M. Bello, G. Moschini, and N. Uzunov, *J. Phys. Conf. Ser.* **253**, 012025 (2010).
- [19] J. Azorin, T. Rivera, C. Falcony, E. Martinez, and M. García, *Radiation protection dosimetry* **85**, 317 (1999).
- [20] Supplemental material.
- [21] S. R. Waitukaitis and H. M. Jaeger, *Rev. Sci. Instrum.* **84**, 025104 (2013).
- [22] T. Pätz, H. J. Herrmann, and T. Shinbrot, *Nat. Phys.* pp. 1–6 (2010).
- [23] J. Randall and M. Wilkins, *P. Roy. Soc. A-Math. Phys.* **184**, 365 (1945).
- [24] M. J. Aitken, *Thermoluminescence Dating* (Academic Press, 1985).
- [25] S. L. Forman, in *Quaternary Geochronology: Methods and Applications*, edited by J. S. Noller, J. M. Gowers, and W. R. Lettis, American Geophysical Union (AGU Books, 2000), pp. 157–176.
- [26] G. Freier, *J. Geophys. Res.* **65**, 3504 (1960).
- [27] A. K. Kamra, *J. Geophys. Res.* **77**, 5856 (2007).
- [28] J. F. Kok and N. O Renno, *Phys. Rev. Lett.* **100**, 014501 (2008).
- [29] D. Schmidt, R. Schmidt, and J. Dent, *J. Geophys. Res.* **103**, 8997 (1998).
- [30] W. R. Harper, *P. Roy. Soc. A-Math. Phys.* **205**, 83 (1951).
- [31] J. Lowell, *J. Phys. D Appl. Phys.* **8**, 53 (1975).
- [32] C.-Y. Liu and A. J. Bard, *Chem. Phys. Lett.* **485**, 231 (2010).
- [33] C.-Y. Liu and A. J. Bard, *J. Am. Chem. Soc.* **131**, 6397 (2009).
- [34] C.-Y. Liu and A. J. Bard, *Chem. Phys. Lett.* **480**, 145 (2009).
- [35] S. Pence, V. Novotny, and A. Diaz, *Langmuir* **10**, 592 (1994).
- [36] L. S. McCarty and G. M. Whitesides, *Angew. Chem. Int. Edit.* **47**, 2188 (2008).
- [37] H. T. Baytekin, A. Z. Patashinski, M. Branicki, B. Baytekin, S. Soh, and B. A. Grzybowski, *Science* **333**, 308 (2011).
- [38] A. F. Diaz, *J. Adhes.* **67**, 111 (1998).
- [39] T. Shinbrot, T. S. Komatsu, and Q. Zhao, *Europhys. Lett.* **83**, 24004 (2008).
- [40] J. A. Wiles, M. Fialkowski, M. R. Radowski, G. M. Whitesides, and B. A. Grzybowski, *J. Phys. Chem. B* **108**, 20296 (2004).